Article

Cell Reports

Live Imaging of HIV-1 Transfer across T Cell Virological Synapse to Epithelial Cells that Promotes Stromal Macrophage Infection

Graphical Abstract

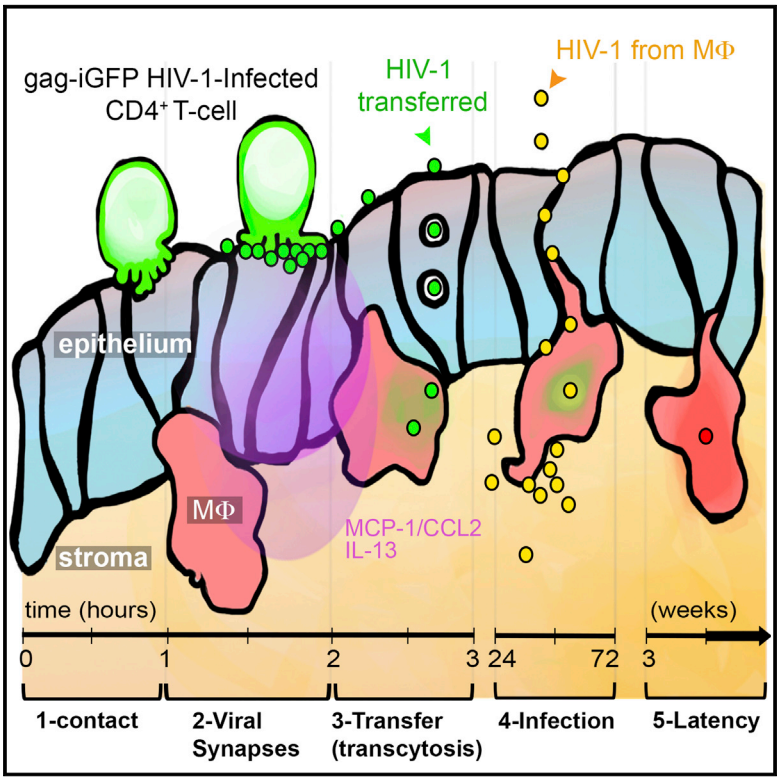

Authors

Fernando Real, Alexis Sennepin, Yonatan Ganor, Alain Schmitt, Morgane Bomsel

Correspondence

morgane.bomsel@inserm.fr

In Brief

Real et al. established by live imaging the dynamics of virological synapses formed between HIV-1-infected T cells and the epithelium at the surface of a human reconstructed mucosa. HIV-1 virions formed at the viral synapse cross the epithelium and reach the mucosal stroma, where the virus establishes a latent infection in macrophages.

Highlights

- HIV-1-infected T cells form viral synapse with the epithelium in reconstructed mucosa
- These viral synapse dynamics were recorded by live imaging for the first time
- HIV-1 formed at the viral synapse crosses the epithelium by transcytosis
- Transcytosed HIV-1 targets stromal macrophages, resulting in their latent infection

Real et al., 2018, Cell Reports *23*, 1794–1805
May 8, 2018 © 2018
https://doi.org/10.1016/j.celrep.2018.04.028

CellPress

OPEN ACCESS
CellPress

Cell Reports
Article

Live Imaging of HIV-1 Transfer across T Cell Virological Synapse to Epithelial Cells that Promotes Stromal Macrophage Infection

Fernando Real,[1,3,4] Alexis Sennepin,[1,3,4] Yonatan Ganor,[1,3,4] Alain Schmitt,[2,3,4] and Morgane Bomsel[1,3,4,5,*]
[1]Laboratory of Mucosal Entry of HIV and Mucosal Immunity, 3I Department, Institut Cochin, Université Paris Descartes, Sorbonne Paris Cité, 75014 Paris, France
[2]Electron Microscopy Facility, Cochin Institute, Paris Descartes University, Sorbonne Paris Cité, 75014 Paris, France
[3]CNRS, UMR8104, 75014 Paris, France
[4]INSERM, U1016, Institut Cochin, 75014 Paris, France
[5]Lead Contact
*Correspondence: morgane.bomsel@inserm.fr
https://doi.org/10.1016/j.celrep.2018.04.028

SUMMARY

During sexual intercourse, HIV-1 crosses epithelial barriers composing the genital mucosa, a poorly understood feature that requires an HIV-1-infected cell vectoring efficient mucosal HIV-1 entry. Therefore, urethral mucosa comprising a polarized epithelium and a stroma composed of fibroblasts and macrophages were reconstructed *in vitro*. Using this system, we demonstrate by live imaging that efficient HIV-1 transmission to stromal macrophages depends on cell-mediated transfer of the virus through virological synapses formed between HIV-1-infected CD4$^+$ T cells and the epithelial cell mucosal surface. We visualized HIV-1 translocation through mucosal epithelial cells via transcytosis in regions where virological synapses occurred. In turn, interleukin-13 is secreted and HIV-1 targets macrophages, which develop a latent state of infection reversed by lipopolysaccharide (LPS) activation. The live observation of virological synapse formation reported herein is key in the design of vaccines and antiretroviral therapies aimed at blocking HIV-1 access to cellular reservoirs in genital mucosa.

INTRODUCTION

The early steps of HIV-1 acquisition during sexual intercourse in men and the establishment of HIV-1 cell reservoirs at the male genital tract are poorly understood features of HIV-1 pathogenesis. The apparent protection against HIV-1 conferred by circumcision (around 50% of reduction) (Auvert et al., 2005) is far from being complete, pointing to the existence of other penile tissues serving as HIV-1 entry sites. The penile urethra is the initial site of infection by many bacterial/viral pathogens that commonly infect the male genital tract, such as *N. gonorrhea*, *C. trachomatis*, *E. coli*, cytomegalovirus, human papilloma virus, and herpes simplex virus-2, demonstrating that the urethral mucosa is accessible to pathogen entry and invasion during sexual intercourse (Pudney and Anderson, 1995). Experiments with the simian immunodeficiency virus (SIV) revealed that infusion of this virus into the urethra of male macaques resulted in the development of acquired immunodeficiency syndrome-like disease, suggesting that the urethral mucosa is also an efficient entry site for HIV-1 (Ma et al., 2016; Miller et al., 1989).

Urethral mucosa displays CD4$^+$ T cells and macrophages as main HIV-1 cell targets, covered by a single thin layer of epithelial cells. Additionally, the expression of mRNA for HIV-1 cellular co-receptors CXCR4 and CCR5 was detected in urethral swabs (Ganor and Bomsel, 2011), thus characterizing the male urethra as a potential entry and establishment site for HIV-1. Accordingly, we have previously shown that HIV-1 efficiently penetrates the urethral mucosa reaching urethral macrophages that in turn traffic from the epithelial to the dermal compartment, in a mechanism controlled by HIV-1-induced cytokines (Ganor et al., 2013). In contrast with foreskin where HIV-1 targets Langerhans cells (Ganor et al. 2010), in the urethral epithelia—in which Langerhans cells are absent—HIV-1 targets macrophages, sparing urethral T cells from infection (Ganor et al., 2013). Therefore, the urethra represents an excellent model of genital mucosa for the study of HIV-1 transmission specific to tissue macrophages, from which productive infection and further dynamics have not been assessed yet.

Once initial infection foci are established, HIV-1 rapidly forms cell reservoirs that cannot be eradicated despite combined antiretroviral treatment. Apart from the best described CD4$^+$ T cell reservoir, HIV-1 establishes myeloid cell reservoirs in tissues constituting an additional obstacle to virus eradication (Honeycutt et al., 2017; Stevenson, 2015). In addition, the vast majority of sexually transmitted HIV-1 uses the CCR5 co-receptor, being thus R5 tropic or macrophage tropic, the variants that predominate in newly transmitted HIV-1 infection (Keele et al., 2008; Margolis and Shattock, 2006). Therefore, CCR5-expressing cells like macrophages would represent a very likely first HIV-1 target during sexual transmission, gaining increasing importance as actors of HIV-1 persistence independently of CD4$^+$ T cells (Honeycutt et al., 2017). At least *in vitro*,

macrophages have a self-limiting production of new viral particles throughout time post-infection, interrupting or keeping a very low-level production after weeks and limiting viral lytic egress and cell-cell spread (Carter and Ehrlich, 2008; Cassol et al., 2009), indicating that macrophages may be important long-lasting reservoirs for the virus.

How HIV-1 reaches these safe niches, established in immune cells such as T cells or Langerhans cells or macrophages depending on the mucosa (Ganor et al., 2013; Hladik and McElrath, 2008; Shen et al., 2009), in the midst of stromal mucosal cells, sheltered from foreign aggressions by the efficient barrier of epithelial cells, remains an open question.

HIV-1 gains access to the body by crossing epithelial barriers that compose the ano-rectal and female/male genital mucosa during sexual intercourse. One pathway of HIV-1 entry at mucosal sites is via transcytosis through epithelial cells after the formation of cell-cell contacts between epithelial cells and HIV-1-infected cells (Alfsen et al., 2005; Bomsel, 1997) present in all secretions that act as vector for HIV-1 infection (Politch et al., 2014). The contact between HIV-1-infected cells and monostratified epithelial target cells triggers the polarized budding of cell-free HIV-1 in a cleft at the site of cell-to-cell contact. Viral particles are then rapidly internalized and transcytosed by the epithelial cells toward the basal pole without infecting epithelial cells, culminating in the release of infectious HIV-1 into the basal environment (Bomsel and Alfsen, 2003; Bomsel, 1997). Next, viruses reach immune cell targets in the stroma and establish infection. In contrast, cell-free HIV-1 inoculated on the epithelial surface transcytoses poorly (Alfsen et al., 2005; Anderson et al., 2010b; Ganor et al., 2010, 2013). Thus, transcytosis and establishment of HIV-1 initial foci at mucosal sites depend on HIV-1 cell-mediated infection, and they occur after the formation of virus-containing clefts, a feature of virological synapses. However, this sequence of events was mainly inferred from biochemical studies or microscopy performed on fixed cells. Furthermore, the dynamic evidence resulting from observations in real time and at a single-cell level that are required for demonstrating virological synapse formation with non-immune target cells, such as epithelial cells, in the context of viral transmission to mucosa, has never been obtained.

Virological synapses are transient and polarized zones of contact between HIV-1-infected and non-infected cells in which viral particles are formed extemporaneously, concentrate, and are transferred from cell to cell. At least *in vitro*, HIV-1 cell-to-cell transmission between immune cells occurs by virological synapses and polysynapses between donor, here HIV-1-infected, cells and one or several target immune cells. This dynamic phenomenon in its essence has been successfully assessed by live-imaging microscopy (Gousset et al., 2008; Hübner et al., 2009; Jolly et al., 2004; Rudnicka et al., 2009; Wang et al., 2017).

Here, using urethral mucosa reconstructed *in vitro*, we describe by quantitative 3D live microscopy the transfer of HIV-1 across T cell virological synapses toward the epithelial cell surface and subsequent mucosal penetration, and we demonstrate that efficient HIV-1 transmission to mucosal tissue macrophages is mediated by virological synapses formed between infected $CD4^+$ T cells and genital mucosa epithelial cells.

RESULTS

Infected $CD4^+$ T Cells Shed HIV-1 on the Mucosal Epithelium Reconstructed *In Vitro*

To monitor the virological synapse in the context of human mucosa and subsequent HIV-1 translocation across polarized epithelial cells, a polarized urethral epithelium was reconstructed *in vitro* and inoculated at its mucosal pole with $CD4^+$ T cells expressing a fluorescent R5-tropic HIV-1 strain (gag-iGFP HIV-1). Human urethral tissue reconstruction consists in the sequential seeding on membrane filters of fibroblasts embedded in collagen matrix together with macrophages, prelabeled with engulfed fluorescent quantum dots, for 2 days forming the stroma. The stroma is overlayed by urethral epithelial cells allowed to grow on the stromal matrix in liquid-liquid and air-liquid environments each for an additional 7 days (Figure 1A). The tissue reconstructions mimic structurally and immunologically the human urethral mucosa, displaying a stroma rich in collagen fibrils (Figure 1B) and a polarized epithelium presenting active caveolar endocytosis and epithelial cell junctions (Figure 1C). The epithelium expresses cytokeratins 10 and 13, allowing for the clear separation of epithelial and stromal regions, the latter containing scattered macrophages vizualized as they were loaded with quantum dots before being inserted in the tissue reconstuction (Figure 1D).

When inoculated selectively at the mucosal pole of the urethral epithelium for 3 hr prior to fixation and observation by confocal microscopy, the $CD4^+$ T cells infected with gag-iGFP HIV-1 interacted exclusively with the surface epithelium, without migrating toward the stroma (Figure 1E). After 3 hr of interaction between HIV-1-infected $CD4^+$ T cells and the urethral mucosa, 17.1% of gag-iGFP HIV-1-infected cells (6 of 35 cells observed) shed fluorescent virus at zones of infected T cell-epithelial cell contact, indicating virological synapses (Figures 1E and 1F).

Transfer of HIV-1 to the Mucosal Epithelium Is Mediated by Virological Synapses

To characterize dynamically the formation of virological synapses formed between HIV-1-infected $CD4^+$ T cells and mucosal epithelial cells, we assessed their interaction by quantitative live imaging from 15 min to 6 hr. Therefore, mucosal tissues were reconstructed on the underside of the membrane filters using the same protocol as above, flipped back to the normal orientation, and inoculated with infected $CD4^+$ T cells deposited on microscopy imaging dishes coupled to an adaptor suitable for microscopy (Figures 2A and 2B). Virological synapses were characterized using the morphological criteria established previously (Hübner et al., 2009), namely, (1) detection of stable (>10-min) organization of fluorescent virus into clusters at zones of cell-cell contact, demonstrated by others to be in fact synaptic clefts (Hübner et al., 2009; Wang et al., 2017); and (2) detection of subsequent transfer of fluorescent virus from the clusters to the target cell.

Upon HIV-1-infected $CD4^+$ T cell-epithelial cell contact, fluorescent viruses, defined by groups of singular fluorescent dots of 0.77 (±0.05 SEM) μm^2 of area, clearly distinguishable from the background, formed and clustered in zones of contact between infected $CD4^+$ cells and epithelial cells. Strikingly, a directional transfer of virus toward epithelial cell surface followed the clustering (Figures 2C and 2D, arrowheads; Videos S1 and S2).

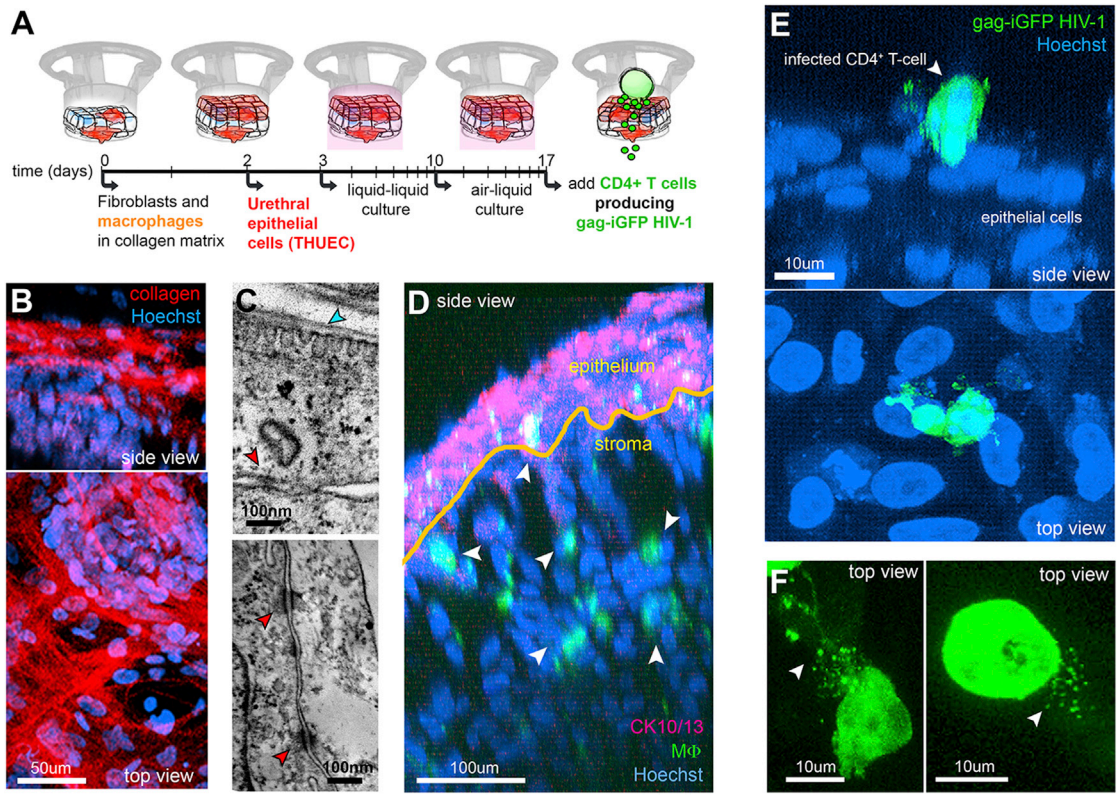

Figure 1. HIV-1-Infected CD4⁺ T Cells Shed Virus on Polarized Urethral Epithelium upon Cell-Cell Contact

(A) Reconstruction of mucosal tissue. Human foreskin primary fibroblasts and monocyte-derived macrophages (MΦ) tagged with fluorescent cell trackers were embedded in the extracellular matrix and seeded on a two-chamber unit membrane for 2 days, subsequently covered by urethral epithelial cells (THUECs) and cultivated for 2 weeks in liquid-liquid then air-liquid environment in a culture medium favoring epithelial polarization. HIV-1-infected T cells producing fluorescent viruses were added on the mucosal side of reconstructed mucosa to initiate infection.

(B) Collagen fibrils (red) in reconstructed urethral mucosa, detected by second harmonics generation (cell nuclei stained with Hoechst in blue). Side and top views are shown. Scale bar, 50 μm.

(C) Electron microscopy images of reconstructed urethra, revealing the presence of caveolae (cyan arrowhead) and desmosomes (red arrowheads) in the epithelium. Scale bar, 100 nm.

(D) Macrophages (arrowheads) distributed in the stroma of reconstructed mucosae (side view). Epithelium and stromal regions were separated by the yellow line, defined after cytokeratin 10/13 expression, in pink. MΦ is shown in green (quantum dot fluorescence), and nuclei are shown in blue (Hoechst). Scale bar, 50 μm.

(E) Side and top views of an HIV-1-infected CD4⁺ T cell producing fluorescent viruses (green) interacting with reconstructed urethral epithelium (nuclei stained with Hoechst in blue).

(F) Two HIV-1-infected CD4⁺ T cells interacting with the epithelium (top view) and shedding fluorescent viruses to the epithelium (arrowheads). Scale bar, 10 μm. Results are representative of n = 2 independent experiments.

The time-spotting of cluster and transfer events (Figure 2E) revealed that transfer of virus starts 37.75 (±14.9 SEM) min after clustering, and transfer events were detected during a mean period of 56.75 min (±12.9 SEM). HIV-1-infected CD4⁺ T cells transferred virus to the urethral epithelium through virological synapse formation in 35.1% of the recorded cells (Table 1), and synapses were resolved after transfer started in 72.7% of the recordings where viral transfers occurred (Figure 2E).

Concerning distinctive features of virological synapses formed between HIV-1-infected T cells and epithelial cells as compared with virological synapses formed with uninfected target CD4⁺ T cells (Figure S1A) or macrophages (Figure S1B; Video S3), we observed (1) the formation of membrane extensions in regions of viral clustering at cell-cell contact zones and from which viral particles were transferred to epithelium; and (2) the transfer of virus that could move away microns of distance from viral synapses regions, not being necessarily retained in viral synapse regions as in the case of bounded synaptic clefts. Frequency of virological synapse formation with epithelial cells in tissue reconstructions was similar to that obtained when uninfected macrophages were targeted. Viral synapse formation followed by virus transfer depended on the HIV-1 envelope, as no transfer to epithelium was observed when a virus mutant lacking the HIV-1 envelope, namely ΔENV, gag-iGFP virus was employed (Video S8; Table 1).

To track macrophages that eventually migrated to upper regions of the epithelium, directly contacting infected CD4⁺ T cells, macrophages were loaded with quantum dots before being inserted into tissue reconstruction. In most of regions where viral synapses were recorded, macrophages were absent or not reaching infected CD4⁺ T cells. In a few recorded cases (n = 3), macrophages

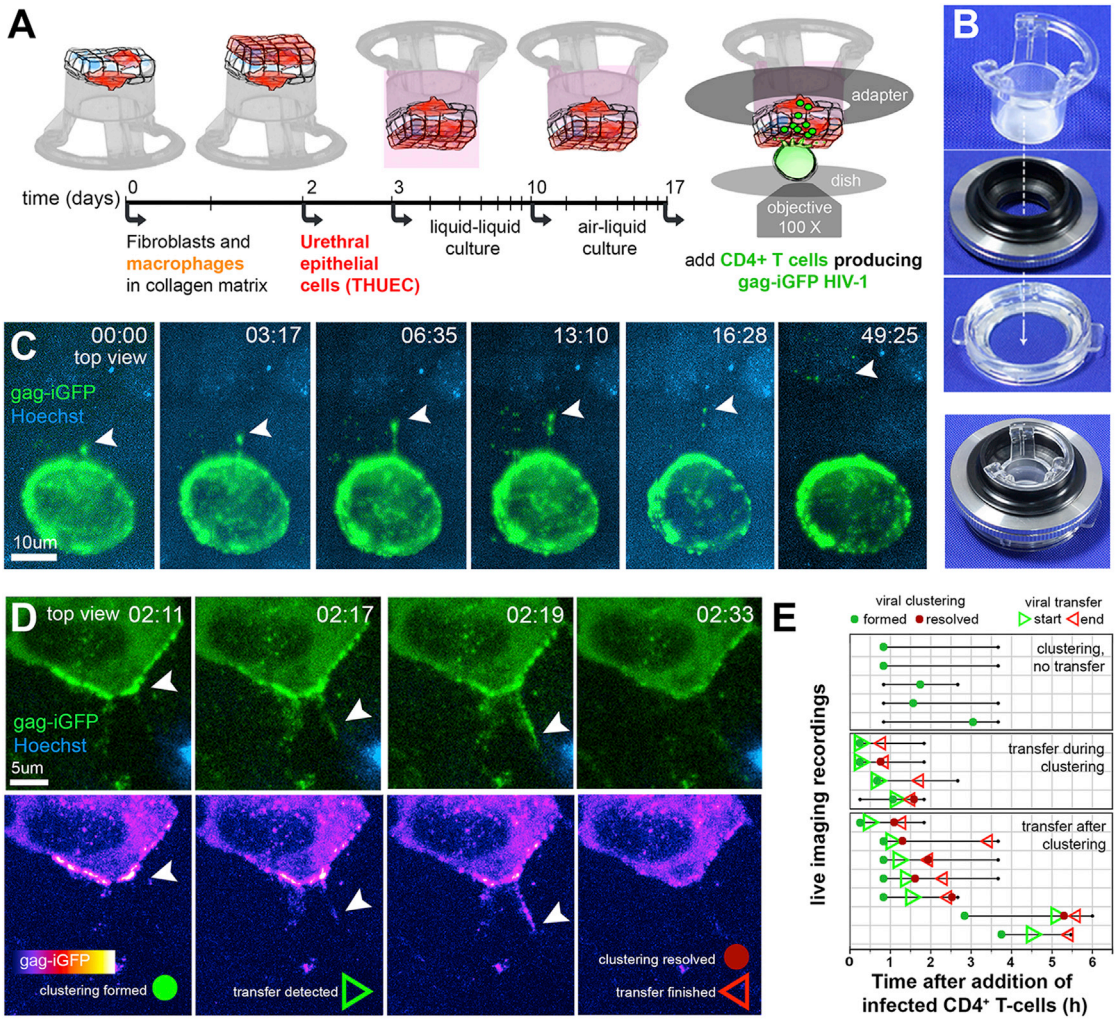

Figure 2. Tracking of HIV-1-Infected T Cell Virological Synapses with the Urethral Epithelium

(A) Reconstruction of mucosal tissue for live-imaging recordings: Tissues were reconstructed on the underside of the chamber membrane filter and incubated at their mucosal pole with HIV-1-infected $CD4^+$ T cells.

(B) The interaction is allowed in a system composed of the membrane filter coupled to an adaptor placed on a microscope dish containing the infected cells. The adaptor adjusts the optical distance between epithelium and high-magnification objectives of the inverted confocal microscope. The upper photograph depicts how the system is mounted (as indicated by the arrow), and the lower photograph shows the ensemble ready for live imaging.

(C and D) HIV-1-infected $CD4^+$ T cells interacting with reconstructed urethral epithelium, as observed by live confocal imaging (infected $CD4^+$ T cell producing gag-iGFP HIV-1 in green; nuclei stained with Hoechst in blue). See also Videos S1 and S2. In (D), gag-iGFP fluorescence is also shown with hue-saturation-value scale ranging from dark blue (less fluorescence) to white (more fluorescence). Detection of viral cluster formation and resolution and the start and end of viral transfers are depicted as green and red circles and green and red triangles, respectively. Time of image acquisition is expressed as minutes:seconds in (C) and hours:minutes in (D). Scale bar, 10 or 5 μm.

(E) Time tracking of virological synapses. Each line in the y axis represents one live-imaging recording, and events of viral clustering (formation, green circle; resolution, red circle) and viral transfers (start, green triangle; end, red triangle) were plotted on the x axis according to the recorded time after interaction with HIV-1-infected $CD4^+$ T cells (hours). Virus is transferred either immediately or within ≈40 min after virological synapse formation; transfer events were observed during ≈1 hr. Results are representative of n = 5 independent experiments.

were present in the epithelium close to infected $CD4^+$ T cell-forming viral synapses, although HIV-1 direct transfers from T cell to these macrophages were not detected, whereas such transfer can be observed in single HIV-1-infected $CD4^+$ T cell/uninfected macrophage co-cultures (Figure S1B; Video S3). Therefore, the formation of viral synapses and clear HIV-1 transfers occur exclusively with epithelial cell targets, despite proximity of macrophages to infected $CD4^+$ T cells (Figure S1E; Video S6).

HIV-1 Shed from Viral Synapses Crosses the Epithelium and Reaches the Mucosal Stroma

Considering that cell-to-cell contact, virological synapse formation, and virus transcytosis across epithelium are sequential events in HIV-1 entry into mucosa (Bomsel, 1997), we tracked fluorescent virus shed from virological synapse into epithelial cells (Figure 3). To specifically delineate the epithelial cell plasma membrane, we constructed urethral epithelial

Table 1. Summary of Detected Virological Synapses Formed between gag-iGFP HIV-1-Infected CD4⁺ T Cell Donor and Various Target Cells in Live-Imaging Recordings

Target Cell	HIV-1 gag-iGFP Strain	Cells Recorded	Virological Synapses	Examples	n	%
Primary CD4⁺ T cells	WT	8	7	Figure S1A	2	87.5
	ΔENV	6	0	data not shown	2	0
MD-MΦ	WT	36	11	Figure S1B; Video S3	5	30.5
	ΔENV	4	0	data not shown	2	0
Urethral epithelial cells	WT	37	13	Figures 2, 3, and S1E; Videos S1, S2, S4, S5, and S6	5	35.1
	ΔENV	5	0	Video S8	2	0

The efficiency of gag-iGFP HIV-1 (wild-type or a mutant virus lacking HIV-1 envelope [ΔENV]) in forming viral synapses and transfer viral particles to target cells was evaluated using target cells such as uninfected primary CD4⁺ cells, peripheral blood monocyte-derived macrophages (MD-MΦ), and urethral tissue reconstructions. n = independent experiments.

cells tagged with red fluorescent ARF6 (ADP-ribosylation factor 6), a protein known to be expressed at the apical plasma membrane of polarized epithelial cells (Altschuler et al., 1999). Using mucosa reconstructed with fluorescent ARF6-tagged epithelial cells and inoculated with HIV-1-infected CD4⁺ T cell in a polarized manner as in Figure 2, we confirmed the direct transfer of HIV-1 from virological synapse to the epithelium (Figure 3A; Video S4). Fluorescent viruses are produced extemporaneously by infected CD4⁺ T cells upon virological synapse establishment, forming clusters in cell-cell contact zones (Figure 3A) corresponding to previous observation with other CD4⁺ T cells (Hübner et al., 2009; Wang et al., 2017). HIV-1 could be detected in intracellular epithelial cell compartments during 3 hr of interaction with HIV-1-infected CD4⁺ T cells when observed at the ultrastructural level by electron microscopy (Figure 3B). Furthermore, the ultrastructure of particles found in epithelial cells was compared with that of HIV-1 particles produced by gag-iGFP HIV-1-infected CD4⁺ T cells, confirming their HIV-1 nature (Figure 3C).

Fluorescent viruses shed following viral synapse formation with the epithelium were then tracked by live imaging in z dimension. Epithelial and HIV-1-infected CD4⁺ T cells were also tracked, and their displacements in z coordinate were used as references for fluorescent virus directional migration. We observed that 3 of 9 (≈30%) tracked fluorescent viruses were found to migrate farther from HIV-1-infected CD4⁺ T cell and translocate across epithelial cell toward the mucosal stroma, indicating viral transcytosis across the epithelial barrier following viral synapse formation (Figures 3D and 3E; Video S5).

Stromal Macrophages Are Infected following HIV-1-Infected T Cell Virological Synapse Formation with the Epithelium

Next, having demonstrated that virological synapses formed with epithelial cell surface lead in turn to extemporaneous HIV-1 production and viral translocation resembling transcytosis across epithelial cells as shown above, we assessed whether transcytosed viruses could then productively infect macrophages in the following days after interaction between urethral tissues within the reconstructed mucosa and HIV-1-infected CD4⁺ T cells. In parallel experiments, cell-free virus was instead inoculated selectively on the tissue mucosal pole. Viral production was assessed by weekly collection of 24-hr serosal tissue culture medium (Figure 4A).

We first confirmed the infectiousness of the R5-tropic gag-iGFP HIV-1 to macrophages after co-culture with infected CD4⁺ T cells (Figure S1C) or in macrophage single cultures infected with cell-free gag-iGFP virus that has been previously produced by HIV-1-infected CD4⁺ T cells (Figure S1D). Resulting infected macrophages displayed the characteristic arrest in viral production around 15 days post-infection (p.i.) with cell-free virus (Figure S1D).

The *in vitro* urethral tissue reconstruction successfully mimicked the physical barrier provided by mucosal epithelia to block direct contact between HIV-1-infected CD4⁺ T cells outside the mucosa and stromal macrophages (Figures 1D and 4B). Infected CD4⁺ T cells did not cross the epithelial barrier, remaining localized above the epithelial layer, as recorded by live imaging (Figure S2A; Video S7). Furthermore, after being washed out from tissue reconstructions at the end of the interaction period, HIV-1-infected CD4⁺ T cells were not detected in the reconstructed mucosa, as in tissue cell suspensions prepared up to 13 days post-infection lacked infected T cells, as demonstrated by flow cytometry (Figure S2B).

When cell-free viruses were added to urethral reconstructions and interacted with the mucosal pole of the epithelium, no viral production was detected in the serosal medium up to 26 days following inoculation (p.i.) (Figure 4C, open circles). Doubling the number of macrophages inserted into the reconstruction had no effect on mucosal infection. This indicates that cell-free viruses were inefficient in targeting macrophages, in agreement with the low efficiency of cell-free HIV-1 to penetrate mucosal epithelia (Alfsen et al., 2005; Anderson, 2014; Bomsel, 1997; Ganor et al., 2013). In contrast, when R5-tropic gag-iGFP HIV-1-infected T cells where inoculated into the mucosal reconstruction in a cell-mediated fashion, viral production was detected up to 18 days p.i. in the serosal medium (Figure 4C, closed circles). Viral production was proportional to the number of macrophages inserted in the reconstruction (Figure 4C, blue and magenta circles), establishing that the detected virus was indeed produced by macrophages inserted in the reconstructed mucosa.

At later time points (up to day 25), viral production became undetectable, suggesting that HIV-1 infection of macrophages had become latent. Latent HIV-1 infection in macrophages was ascertained using lipopolysaccharide (LPS), a molecule known to re-activate viral production from latency specifically in

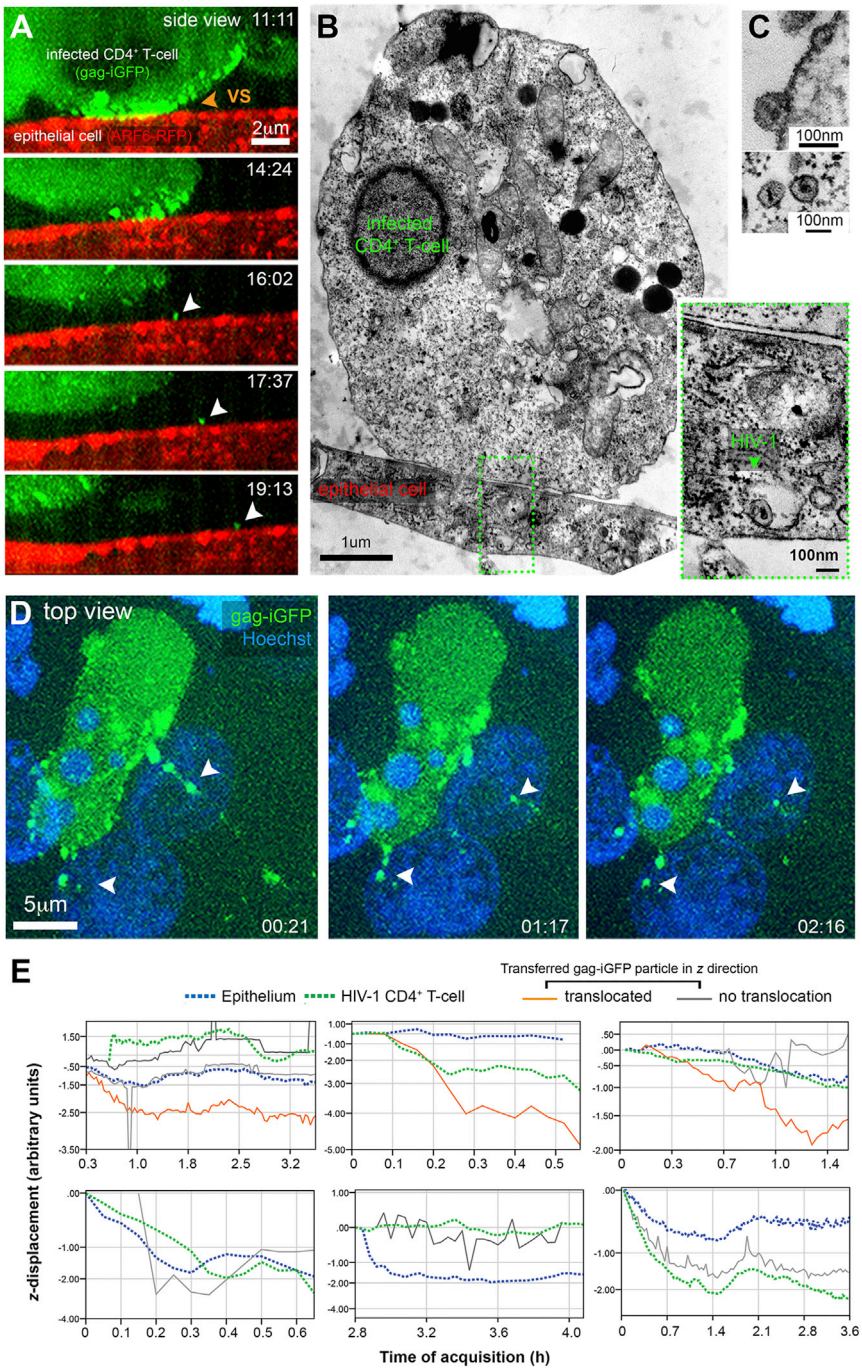

Figure 3. Viral Particles Formed at the Virological Synapse Transcytose across the Epithelium toward the Mucosal Stroma

(A) HIV-1-nfected CD4$^+$ T cell (fluorescent virus in green) interacting with epithelium (THUECs engineered to express a fluorescent ARF6 GTPase at the apical plasma membrane to delineate the cell border in red). Clustering and shedding of fluorescent virus at the zone of contact are indicated by arrowheads. Time of image acquisition is depicted as minutes:seconds. Scale bar, 5 µm. Results are representative of 3 virological synapses with ARF6-tagged THUEC recorded in n = 3 independent experiments. See also Video S4.

(B) Contact zone between infected CD4$^+$ T cell and epithelium imaged by electron microscopy. The green dotted square region shown in high magnification (inset) reveals a viral particle within an epithelial cell compartment. Scale bars, 1 µm and 100 nm.

(C) Examples of viral particles shed by an infected CD4$^+$ T cell under electron microscopy. Scale bar, 100 nm.

(D) Live imaging of an infected CD4+ T cell forming a virological synapse and transferring viruses to epithelium; arrowheads in the sequence indicate examples of particles tracked for vertical (z coordinate) displacement in (E). Time, hours:minutes; scale bar, 10 µm. See also Video S5. Results are representative of 13 virological synapses recorded in n = 5 independent experiments.

(E) Vertical (z coordinate) tracking of fluorescent virus shed from a virological synapse. Displacement in z coordinate of epithelial cells (blue dotted line), infected CD4$^+$ T cell (green dotted line), and transferred gag-iGFP particles (gray, not displaced; orange, displaced in z direction). Displacement was calculated by subtracting the z coordinate at each time point by the initial z coordinate at time point = 0. Negative values represent displacement toward tissue reconstructions, while positive values represent displacement toward the confocal unit objective. From 6 different live recordings analyzed in n = 4 independent experiments, 3 of 9 tracked gag-iGFP particles migrate further in z toward the stroma, thus indicating transcytosis.

infected macrophages (Liou et al., 2002; Pomerantz et al., 1990). Hence, treatment with LPS at day 25 p.i. of reconstruction otherwise arrested in viral production induced a viral rebound, as compared with non-treated reconstructions (Figure 4C, graph on the right).

Macrophages were retained in urethral mucosal reconstructions after long-term cell-mediated HIV-1 infection, although their location remained restricted to stromal regions at later time points p.i. (Figure 4D). *In situ* hybridization performed using the recently developed DNA/RNA scope technology (Deleage et al., 2016) revealed that tissular macrophages displayed integrated proviral DNA as early as 3 days p.i. Furthermore, HIV-1 DNA was detected exclusively in macrophages colabeled with CD68, not epithelial cells (Figure 4E, arrowheads). At long-term infection, when macrophages were latently infected, e.g., 25 days p.i., HIV-1 capsid proteins were detected in intracellular clusters within CD68$^+$ macrophage, as shown by immunofluorescent labeling observed by confocal microscopy (Figure 4F), suggestive of viral-containing compartments typical of HIV-1 infection in myeloid cells (Rodrigues et al., 2017) (unpublished data).

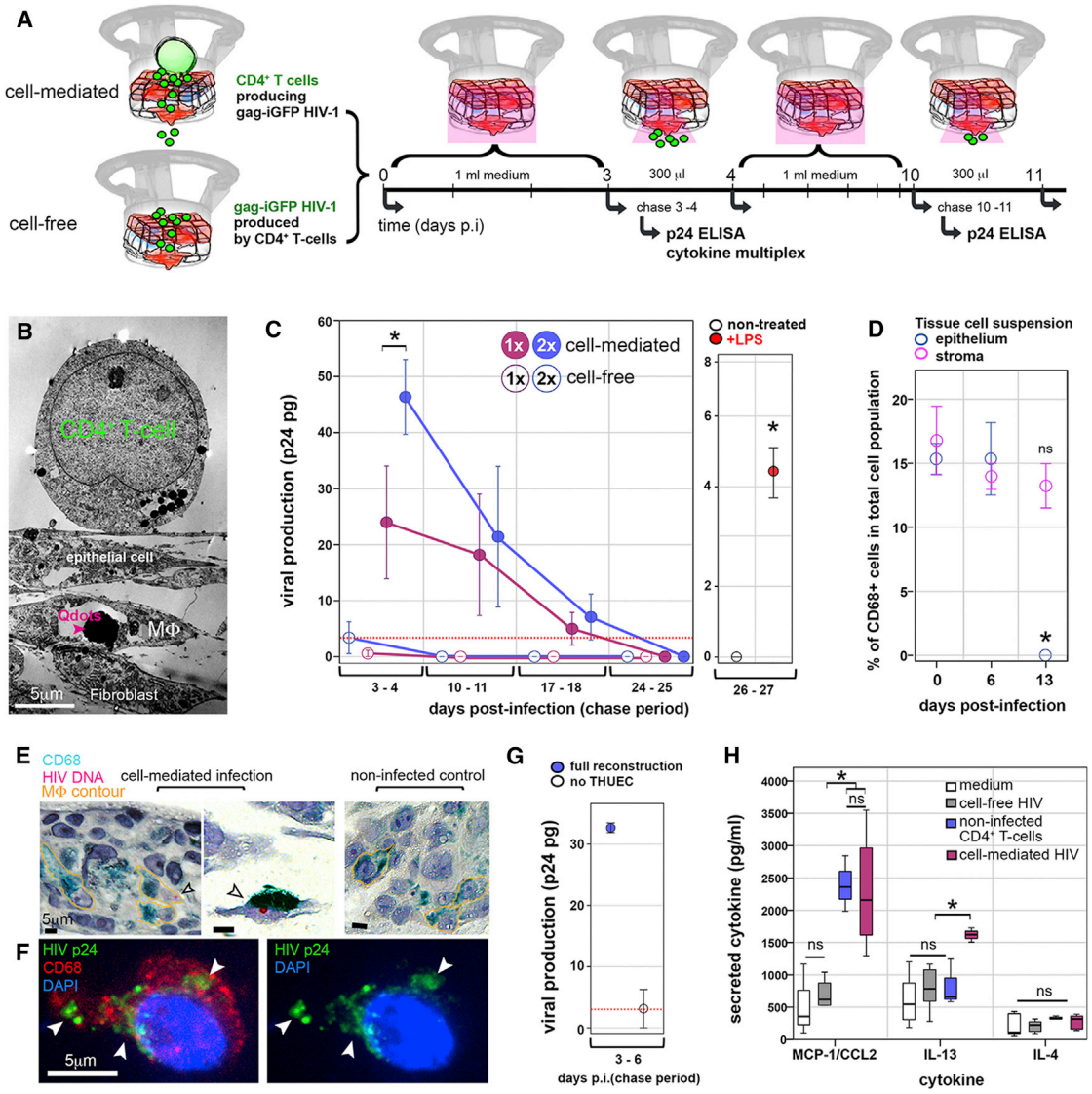

Figure 4. Virological Synapses with the Epithelium Mediate HIV-1 Infection of Tissue Macrophages

(A) Experimental set-up for cell-mediated or cell-free virus infection of reconstructed mucosa. After 2 hr of interaction with HIV-1-infected CD4$^+$ T cells or cell-free viruses, 24-hr tissue supernatants (chase period) were collected at different indicated time points throughout 28 days post-infection (p.i.), chase periods being separated by a resting period of 1 week of cultivation.

(B) HIV-1-infected CD4$^+$ T cell contacting reconstructed mucosal epithelial cells, but not macrophages (MΦ, identified by electron-dense quantum dots (Qdots) indicated by a red arrowhead), as observed by electron microscopy. Scale bar, 5 µm.

(C) MΦ viral production after cell-free versus cell-mediated infection of reconstructions containing different amounts (1× or 2×) of inserted MΦ. Treatment of the reconstruction with 1 µg/mL LPS restored viral production during the chase period between 26 and 27 days p.i. The limit of p24 detection is shown by the red dotted line. Results are representative of n = 3 independent experiments. Data are represented as mean ± SEM; *p < 0.05 (ANOVA).

(D) Flow cytometry analysis of the percentage of CD68$^+$ cells in the total population of cells of epithelium and stroma tissue cell suspensions. Macrophages are retained in the stroma after 13 days post-infection, whereas no macrophages were detected in the epithelium at this later time point. Data are represented as mean ± SEM; *p < 0.05 (ANOVA); ns, non-significant.

(E) HIV-1 DNA *in situ* hybridization (ISH) of infected (cell-mediated) and non-infected (control) tissue reconstructions. Proviral DNA staining is shown in magenta and CD68 co-stainning is shown in cyan (HistoGreen staining), allowing contour of CD68+ macrophages in yellow. Proviral DNA is only detected in CD68$^+$ macrophages early after 3 days of cell-mediated infection (two first images). Arrowhead indicates infected macrophage. Scale bar, 5 µm.

(F) Double indirect immunofluorescence of HIV-1 capsid proteins (p24) observed by confocal microscopy is only detected in CD68$^+$ macrophages, in the stroma of tissue reconstructions infected for 25 days. CD68 staining, red; p24 staining, green; nucleus staining, blue (DAPI). Arrowheads point to clusters of viral proteins, indicating viral-containing compartments. Scale bar, 5 µm.

(legend continued on next page)

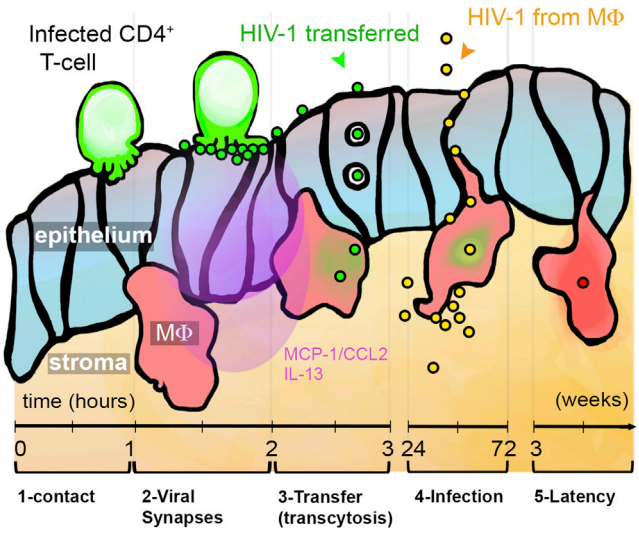

Figure 5. Chain of Events of HIV-1 Transmission to Macrophages in Genital Tissue following Virological Synapse Formation

After contacting the epithelium (1), HIV-1-infected CD4$^+$T cells locally transfer the virus through virological synapses (2) followed by viral transcytosis (3). Macrophages are efficiently targeted in a microenvironment rich in macrophage chemoattractant cytokine MCP-1/CCL2 (induced by contact between the epithelium and CD4$^+$T cells) and IL-13 (secreted specifically upon virological synapse formation). In turn, macrophages display HIV-1 DNA and produce new viral particles for weeks following infected CD4$^+$T cell interaction with the epithelium (4). Macrophage viral production decreases until latency, reversed by LPS administration (5). Altogether, results demonstrate the potential of mucosal stromal macrophages for establishing viral reservoirs early after infected T cell virological synapses formed with epithelial cells.

Direct cell-mediated HIV-1 infection of target macrophages embedded in the collagen matrix did not occur when tissue reconstructions devoid of epithelial cells interacted with infected CD4$^+$ T cells (Figure 4G), indicating that the epithelial barrier is needed as an active intermediate between HIV-1 cell-mediated inoculation and macrophage targeting. Such an active role of the epithelial barrier resulted from cytokine/chemokine secretion induced by the virological synapse formation. Hence, the interaction between HIV-1-infected CD4$^+$ T cells and epithelium and the formation of virological synapses increased the secretion in the reconstruction culture medium of anti-inflammatory interleukin-13 (IL-13) in the following 3 days p.i. (Figure 4H). Furthermore, the macrophage chemoattractant cytokine MCP-1/CCL2 secretion was increased upon epithelium interaction with CD4$^+$ T cell, although regardless of infection. Other tested cytokines, such as the anti-inflammatory IL-4 (<500 pg/mL; Figure 4H) but also pro-inflammatory ones, were also constitutively secreted by tissue reconstructions at low levels, not modified by viral synapses (MCP-4/CCL13, <100 pg/mL; MIP-3α/CCL20, <40 pg/mL; MIP-1α/CCL3, <500 pg/mL; and RANTES/CCL5 and TRAIL/TNFSF10, <100 pg/mL).

DISCUSSION

We have established a urethral mucosa reconstruction model suitable for live imaging at high-dimensional resolution and appropriate minute-wise temporal resolution, which allowed for the unprecedented demonstration in real time that virological synapses are formed between HIV-1-infected CD4$^+$ T cells and the human genital epithelium, thereby simulating *in vitro* HIV-1 acquisition as it occurs during sexual intercourses.

The scenario of cell-mediated targeting of mucosal macrophages via virological synapses, as demonstrated here using urethral tissue reconstructions infected with R5-tropic HIV-1, is schematized in Figure 5. It comprises the following sequential steps: (1) contact between HIV-1-infected cells vectoring infection and the mucosal epithelial surface; (2) virological synapse formation allowing for extemporaneous virus budding on the epithelial cell layer; (3) HIV-1 translocation in a transcytosis-like process across epithelium toward the mucosal stroma; and, (4) in an anti-inflammatory microenvironment, stromal macrophages being infected, having integrated proviral DNA in their genomes, and producing new viral particles for 3 weeks p.i. prior to (5) the establishment of a reversibly latent macrophage infection.

There is increasing evidence that cell-mediated HIV-1-infected cells are more efficient than cell-free virus for spreading infection to other cell targets (Alfsen et al., 2005; Bomsel, 1997; Bomsel and Alfsen, 2003; Deeks, 2011; Iwami et al., 2015; Sigal et al., 2011), although HIV-1 likely employs both modes of transmission. Efficient transfer following cell-mediated infection is due to the extemporaneous generation of infectious virus concentrated in regions of cell-to-cell contact. The virus is shielded from host cell restriction factors and neutralizing antibodies, especially those directed against the gp120 glycoprotein from the virus envelope (Abela et al., 2012; Kulpa et al., 2013), thereby favoring viral transmission.

Virological synapse in the context of mucosal epithelial cells was inferred before by functional assays regarding the efficiency of cell-associated versus cell-free virus for HIV-1 entry into epithelium and by microscopic observation of fixed samples (Bomsel, 1997; Alfsen et al., 2005; Bouschbacher et al., 2008; Collins et al., 2000; Ganor et al., 2013, 2010; Zussman et al., 2003). We provide direct evidence of virological synapse formation at the mucosal level, retrieved from dynamic observation of the interaction between live HIV-1-infected CD4$^+$ T cells and urethral epithelium. We demonstrate the formation of clusters of fluorescent viruses at zones of synaptic contacts, sustained for $\approx$40 min and followed by viral transfers toward the epithelium. Similar to viral synapses formed between T cells (Hübner et al., 2009), CD4$^+$ T cells infected with an envelope-depleted HIV-1 variant (ΔENV) of fluorescent virus are unable to transfer virus to reconstructed urethral epithelium. This result highlights that an HIV-1 envelope-dependent viral synapse with mucosal epithelial cells occurs independently of CD4 engagement (Zhou

(G) Viral production of 72-hr tissue supernatants (chase period between 3 and 6 days p.i.) after cell-mediated infection of full or incomplete (no THUECs added) reconstructions. Limit of p24 detection is shown by red dotted line. Data are represented as mean ± SEM.

(H) Measurement of MCP-1/CCL2, IL-13, and IL-4 cytokines constitutively secreted by tissue reconstructions or secreted upon interaction of tissues with cell-free HIV-1 or HIV-1-infected or non-infected CD4$^+$ T cells. Data are represented as boxplots; *$p < 0.05$ (ANOVA); ns, non-significant. Results are representative of n = 3 independent experiments.

et al., 2018), likely through glycosphingolipid galactosylceramide (GalCer) expressed on the apical surface of CD4-negative epithelial cells (Alfsen and Bomsel, 2002).

Viral transfers after virological synapses occur for ≈1 hr, and fluorescent HIV-1 transcytoses across epithelial cells in regions where viral synapses form. This time window of synapse between HIV-1-infected T cell and mucosal epithelia is similar to that of viral synapses recorded between HIV-1-infected and non-infected T cells, with a mean duration of 60 min (Martin et al., 2010), and events of virus transfer, which last for 3 hr (Chen et al., 2007; Jolly et al., 2004). It corresponds to the required time for HIV-1 to efficiently translocate through urethral and foreskin epithelia (Ganor et al., 2010, 2013) or endometrial cells (Bomsel, 1997). Contact between infected $CD4^+$ T cells and mucosal epithelium established during the first hour of interaction is required for the subsequent efficient transport of viruses across epithelium to the stroma. In contrast, cell-free viruses that also contact the epithelium are inefficient in crossing mucosal layers of cells and targeting macrophages, in agreement with our and previous studies using different models (Alfsen and Bomsel, 2002; Alfsen et al., 2001, 2005; Bomsel, 1997; Bomsel et al., 1998; Bouschbacher et al., 2008; Ganor et al., 2010, 2013).

In inflammatory conditions, junctions of the epithelial barrier can be loosened, allowing for paracellular cell-free HIV-1 transport (Carreno et al., 2002). Alternatively, in pluristratified mucosa such as the vagina, HIV-1-infected cells could penetrate the epithelium, although a clear definition of HIV-1 entry pathway *in vivo* remains to be ascertained (Bernard-Stoecklin et al., 2014). Therefore, transcytosis is not the sole pathway for the virus to cross the epithelial barrier. We and others have shown that, although the epithelial barrier is not disturbed by the cell-cell contact, no direct contact between submucosal immune cells and HIV-1-infected cells was detected and cell-associated mucosal transcytosis is 50–100 times more efficient than that of cell-free viruses (Alfsen et al., 2005; Anderson et al., 2010a), indicating that HIV-1 transcytosis is one major pathway for cell-mediated penetration across the mucosal epithelia.

The lack of efficient mucosal penetration of cell-free virus also indicates that cell-cell contacts not only participate in local viral production for efficient epithelial uptake but are also actively implicated in later steps of viral entry, such as immunomodulation of mucosal response by transducing signals to epithelial cells, via nuclear factor κB (NF-κB) activation, driving downstream inflammatory signaling events as we recently reported (Zhou et al., 2018) and ultimately the infection of tissue macrophages here reported.

The mucosal epithelium of urethra, like the gastrointestinal and other mucosal tissues, directly interacts with viral and non-viral pathogens, exerting an important and primordial barrier to prevent pathogen access to underlying stromal cells and to blood circulation (Ganor et al., 2013; Pudney and Anderson, 1995). Epithelial cells that either contact or are infected by microbes were shown to respond immunologically to pathogens by engaging pathogen recognition receptors (PRRs). In turn, chemokines and inflammatory mediators are produced that recruit innate and adaptive effector cells, thus orchestrating an early response against an eventual pathogen penetration into the epithelial barrier (Hyun et al., 2015; Nasu and Narahara, 2010; Stanley, 2012; Zhou et al., 2018). Pathogens like HIV-1 have evolved strategies to overcome the epithelial barrier and profit from the immunomodulatory environment triggered by aggressed epithelial cells to spread. For instance, the interaction of T cells expressing the HIV-1 envelope with foreskin keratinocytes engage epithelial cell PRRs, such as Toll-like receptor-4, promoting the secretion of pro-inflammatory cytokines and chemokines known to attract HIV-1 cell targets, including macrophages (Zhou et al., 2018). In this context, epithelial cells respond to HIV-1 virological synapses established with the mucosal epithelial surface by producing chemokines sensed by stromal immune cells, including macrophages, allowing for their migration toward epithelial serosal membrane to capture transcytosed virus, as we suggested (Zhou et al., 2018).

In the present model, virological synapses formed by $CD4^+$ T cells infected with replication-competent HIV-1 with urethral tissue reconstructions induced an increase in the secretion of the macrophage chemoattractant pro-inflammatory cytokine MCP-1/CCL2 and the anti-inflammatory cytokine IL-13. MCP-1/CCL2 secretion is induced upon the interaction between $CD4^+$ T cells and tissue reconstructions, but irrespective of T cell infection. MCP-1/CCL2 is associated with monocyte recruitment to sites of inflammation (Deshmane et al., 2009) and could participate to recruit or maintain target macrophages in the submucosa near the basal membrane, ready to capture HIV-1 exiting the epithelium after transcytosis. IL-13 secretion, on the other hand, is increased specifically upon virological synapse formation, as only HIV-1-infected $CD4^+$ T cells can trigger an upregulated secretion of this cytokine by tissue reconstructions. In this scenario, synapse-dependent IL-13 and MCP-1/CCL2 increased secretion after virological synapse formation promote an anti-inflammatory microenvironment that favors chemoattraction of macrophages to synaptic regions and/or polarizes macrophages toward immunological profiles susceptible for long-lasting viral reservoir formation (Cassol et al., 2009; Saïdi et al., 2010) (unpublished data).

After epithelial transcytosis and release in the stroma, HIV-1 can gain access to macrophages and, in turn, subvert these cells in stable viral reservoirs by promoting integration of viral genome (Cassol et al., 2009), low-level viral replication for days, as demonstrated *in vitro* (Swingler et al., 2007) and *in vivo* using the SIV model (Ribeiro Dos Santos et al., 2011), and latent infection (Cassol et al., 2009; Coiras et al., 2009) (unpublished data). Tissular macrophages display proviral DNA early after 3 days of cell-mediated infection of tissue reconstructions, and we observed a similar self-limiting dynamic of viral production coming from tissue reconstructions throughout the days after cell-mediated infection, proportional to the number of macrophages employed to reconstruct tissues. The latency of macrophage infection, i.e., the reversibly nonproductive state of infection (Eisele and Siliciano, 2012) in the weeks following T cell virological synapses formed with epithelial cells, was demonstrated by restoring viral production of infected macrophages, located mainly in the stroma 13 days p.i., by LPS treatment, which is known to reactivate once silent HIV-1 LTR promoters in a TLR4-mediated process (Liou et al., 2002; Pomerantz et al., 1990).

By simulating the interaction with HIV-1-infected CD4$^+$ T cells with genital mucosal epithelium using tissues reconstructed *in vitro*, the results altogether demonstrate that the establishment of HIV-1 latent infection in mucosal macrophages in the stroma occurs after virological synapses formed first with the epithelial cell barrier. How HIV-1, produced locally at the virological synapse, gets selective access to immune cell targets in the urethra and other genital mucosa and which mechanisms drive the selectivity of the targeting to macrophages are topics currently under investigation.

Overall, the present study addresses basic physiopathology questions on the early mechanism of HIV-1 penetration in male genital mucosa at the cell-biology level. We have demonstrated that virological synapses are formed between an HIV-1-infected donor immune cell and a target epithelial cell in male urethral mucosa, potentially revealing additional aspects of HIV-1 transmission that may contribute to the design of better-targeted antiviral strategies.

EXPERIMENTAL PROCEDURES

Ethics Statement

Foreskin primary fibroblasts and peripheral blood mononuclear cells, obtained from healthy volunteers and supplied, respectively, by the Urology Service at the Cochin Hospital, Paris, France, and the local Blood Center (Établissement Français du Sang), were employed in this study according to local ethical regulation, and methods were approved by a local ethical committee (Comité de Protection des Personnes, CPP, Île de France XI, approval 11,016).

Primary Cells

Primary fibroblasts were obtained from the foreskin of healthy adults undergoing circumcision as described (Ganor et al., 2010). Primary CD4$^+$ T cells were obtained and activated as described (Tudor et al., 2012). Primary macrophages were obtained from monocyte-enriched peripheral blood mononuclear cells (PBMCs), isolated from healthy blood donors and cultivated for 6 days with 25 ng/mL macrophage colony-stimulating factor (M-CSF, R&D Systems) and 50 ng/mL granulocyte macrophage colony-stimulating factor (GM-CSF, R&D Systems).

Infection of Inverted Tissue Reconstructions for Live Imaging

Urethral reconstructions interacting with HIV-1-infected CD4$^+$ T cells expressing fluorescent HIV-1 were observed with a confocal unit coupled to a heating chamber (ibidi) and located in a BSL3 facility. Tissues reconstructed in the inverted fashion were brought to objective lens working distances with the aid of an adaptor for imaging membrane filters (Delta T Artificial Membrane Adaptor, Bioptechs), as reported by others (Ott and Lippincott-Schwartz, 2012; Wakabayashi et al., 2007) and shown in Figure 2B. Delta T was previously adjusted to allow for high-magnification imaging of tissue with minimum contact of the epithelium and the microscopy dish. The nucleic acid cell-permeant probe Hoechst 33258 (Sigma-Aldrich) was added to tissue reconstructions used for live imaging, at a concentration of 25 μg/mL in reconstruction medium for 1 hr in a 37°C 5%-CO_2 environment.

A small volume of RPMI medium with 10% fetal bovine serum (FBS) containing infected CD4$^+$ T cells (50 μL) was placed between the epithelium held by the Delta T adaptor and the microscopy dish (μDish 35 mm, ibidi) coupled to the adaptor. The thin coverglass in the bottom of these chambers (0.13–0.16 mm) allowed for 100 × 1.4-numerical aperture (NA) oil-immersion objective lens to reach the epithelium cell layer of the tissue cultivated on the filter underside. Other lower-magnification objectives (63 × 1.4 NA and 40 × 1.3 NA oil-immersion objectives) were also employed for image acquisition to include more than one infected cell per field, at the expense of spatial resolution.

Live imaging generates three-dimensional reconstructions from confocal optical sections, obtained from live samples at defined time intervals (3D plus time), allowing for spatial and temporal acquisition and statistical analysis of dynamic events, such as viral synapses and HIV-1 translocation in the z direction. At the microscope, the live imaging of reconstructed tissue was performed during up to 2 hr of HIV-1-infected CD4$^+$ T cells and urethral epithelium interaction, aiming to track fluorescent HIV-1 clustered at regions of contact between these cells. With the technique, we tracked live fluorescent and infectious virus in time and in x, y, and z spatial coordinates. Images were acquired by Metamorph 7.7.5 software (Molecular Devices), using low-laser input (3% and 8% of laser potency for laser lines 405 and 491, respectively) and no image binning.

Statistical Analysis

Statistical analysis was performed using SPSS software. The statistical tests were employed based on normal and non-normal distributions and equal and non-equal variances.

SUPPLEMENTAL INFORMATION

Supplemental Information includes Supplemental Experimental Procedures, two figures, and eight videos and can be found with this article online at https://doi.org/10.1016/j.celrep.2018.04.028.

ACKNOWLEDGMENTS

This work was supported by the Agence nationale de recherches sur le sida et les hépatites virales (ANRS) fund (ANRS-2014AO21038) to M.B. F.R. and A. Sennepin were supported by fellowships from SIDACTION and ANRS. We would like to thank the staff of Institut Cochin IMAGI'C and CYBIO facilities and Dr. Benjamin Cheng (Icahn School of Medicine at Mount Sinai, New York, NY) for providing the gag-iGFP HIV-1 plasmids employed in this study.

AUTHOR CONTRIBUTIONS

F.R. and M.B. conceived and analyzed the experiments. F.R. conducted the experiments and performed statistical analyses. Y.G., A. Sennepin, and F.R. established the *in vitro* reconstruction of urethral tissues. A. Schmitt, M.B., and F.R. performed electron microscopy observation and analysis. F.R. and M.B. wrote the manuscript.

DECLARATION OF INTERESTS

The authors declare no competing interests.

Received: October 6, 2017
Revised: February 20, 2018
Accepted: April 4, 2018
Published: May 8, 2018

REFERENCES

Abela, I.A., Berlinger, L., Schanz, M., Reynell, L., Günthard, H.F., Rusert, P., and Trkola, A. (2012). Cell-cell transmission enables HIV-1 to evade inhibition by potent CD4bs directed antibodies. PLoS Pathog. *8*, e1002634.

Alfsen, A., and Bomsel, M. (2002). HIV-1 gp41 envelope residues 650-685 exposed on native virus act as a lectin to bind epithelial cell galactosyl ceramide. J. Biol. Chem. *277*, 25649–25659.

Alfsen, A., Iniguez, P., Bouguyon, E., and Bomsel, M. (2001). Secretory IgA specific for a conserved epitope on gp41 envelope glycoprotein inhibits epithelial transcytosis of HIV-1. J. Immunol. *166*, 6257–6265.

Alfsen, A., Yu, H., Magérus-Chatinet, A., Schmitt, A., and Bomsel, M. (2005). HIV-1-infected blood mononuclear cells form an integrin- and agrin-dependent viral synapse to induce efficient HIV-1 transcytosis across epithelial cell monolayer. Mol. Biol. Cell *16*, 4267–4279.

Altschuler, Y., Liu, S., Katz, L., Tang, K., Hardy, S., Brodsky, F., Apodaca, G., and Mostov, K. (1999). ADP-ribosylation factor 6 and endocytosis at the apical surface of Madin-Darby canine kidney cells. J. Cell Biol. *147*, 7–12.

Anderson, D.J. (2014). Modeling mucosal cell-associated HIV type 1 transmission in vitro. J. Infect. Dis. *210* (*Suppl 3*), S648–S653.

Anderson, D.J., Politch, J.A., Nadolski, A.M., Blaskewicz, C.D., Pudney, J., and Mayer, K.H. (2010a). Targeting Trojan Horse leukocytes for HIV prevention. AIDS *24*, 163–187.

Anderson, D.J., Pudney, J., and Schust, D.J. (2010b). Caveats associated with the use of human cervical tissue for HIV and microbicide research. AIDS *24*, 1–4.

Auvert, B., Taljaard, D., Lagarde, E., Sobngwi-Tambekou, J., Sitta, R., and Puren, A. (2005). Randomized, controlled intervention trial of male circumcision for reduction of HIV infection risk: the ANRS 1265 Trial. PLoS Med. *2*, e298.

Bernard-Stoecklin, S., Gommet, C., Cavarelli, M., and Le Grand, R. (2014). Nonhuman primate models for cell-associated simian immunodeficiency virus transmission: the need to better understand the complexity of HIV mucosal transmission. J. Infect. Dis. *210* (*Suppl 3*), S660–S666.

Bomsel, M. (1997). Transcytosis of infectious human immunodeficiency virus across a tight human epithelial cell line barrier. Nat. Med. *3*, 42–47.

Bomsel, M., and Alfsen, A. (2003). Entry of viruses through the epithelial barrier: pathogenic trickery. Nat. Rev. Mol. Cell. Biol. *4*, 57–68.

Bomsel, M., Heyman, M., Hocini, H., Lagaye, S., Belec, L., Dupont, C., and Desgranges, C. (1998). Intracellular neutralization of HIV transcytosis across tight epithelial barriers by anti-HIV envelope protein dIgA or IgM. Immunity *9*, 277–287.

Bouschbacher, M., Bomsel, M., Verronèse, E., Gofflo, S., Ganor, Y., Dezutter-Dambuyant, C., and Valladeau, J. (2008). Early events in HIV transmission through a human reconstructed vaginal mucosa. AIDS *22*, 1257–1266.

Carreno, M.P., Krieff, C., Irinopoulou, T., Kazatchkine, M.D., and Belec, L. (2002). Enhanced transcytosis of R5-tropic human immunodeficiency virus across tight monolayer of polarized human endometrial cells under pro-inflammatory conditions. Cytokine *20*, 289–294.

Carter, C.A., and Ehrlich, L.S. (2008). Cell biology of HIV-1 infection of macrophages. Annu. Rev. Microbiol. *62*, 425–443.

Cassol, E., Cassetta, L., Rizzi, C., Alfano, M., and Poli, G. (2009). M1 and M2a polarization of human monocyte-derived macrophages inhibits HIV-1 replication by distinct mechanisms. J. Immunol. *182*, 6237–6246.

Chen, P., Hübner, W., Spinelli, M.A., and Chen, B.K. (2007). Predominant mode of human immunodeficiency virus transfer between T cells is mediated by sustained Env-dependent neutralization-resistant virological synapses. J. Virol. *81*, 12582–12595.

Coiras, M., López-Huertas, M.R., Pérez-Olmeda, M., and Alcamí, J. (2009). Understanding HIV-1 latency provides clues for the eradication of long-term reservoirs. Nat. Rev. Microbiol. *7*, 798–812.

Collins, K.B., Patterson, B.K., Naus, G.J., Landers, D.V., and Gupta, P. (2000). Development of an in vitro organ culture model to study transmission of HIV-1 in the female genital tract. Nat. Med. *6*, 475–479.

Deeks, S.G. (2011). HIV: How to escape treatment. Nature *477*, 36–37.

Deleage, C., Wietgrefe, S.W., Del Prete, G., Morcock, D.R., Hao, X.P., Piatak, M., Jr., Bess, J., Anderson, J.L., Perkey, K.E., Reilly, C., et al. (2016). Defining HIV and SIV Reservoirs in Lymphoid Tissues. Pathog. Immun. *1*, 68–106.

Deshmane, S.L., Kremlev, S., Amini, S., and Sawaya, B.E. (2009). Monocyte chemoattractant protein-1 (MCP-1): an overview. J. Interferon Cytokine Res. *29*, 313–326.

Eisele, E., and Siliciano, R.F. (2012). Redefining the viral reservoirs that prevent HIV-1 eradication. Immunity *37*, 377–388.

Ganor, Y., and Bomsel, M. (2011). HIV-1 transmission in the male genital tract. Am. J. Reprod. Immunol. *65*, 284–291.

Ganor, Y., Zhou, Z., Tudor, D., Schmitt, A., Vacher-Lavenu, M.C., Gibault, L., Thiounn, N., Tomasini, J., Wolf, J.P., and Bomsel, M. (2010). Within 1 h, HIV-1 uses viral synapses to enter efficiently the inner, but not outer, foreskin mucosa and engages Langerhans-T cell conjugates. Mucosal Immunol. *3*, 506–522.

Ganor, Y., Zhou, Z., Bodo, J., Tudor, D., Leibowitch, J., Mathez, D., Schmitt, A., Vacher-Lavenu, M.C., Revol, M., and Bomsel, M. (2013). The adult penile urethra is a novel entry site for HIV-1 that preferentially targets resident urethral macrophages. Mucosal Immunol. *6*, 776–786.

Gousset, K., Ablan, S.D., Coren, L.V., Ono, A., Soheilian, F., Nagashima, K., Ott, D.E., and Freed, E.O. (2008). Real-time visualization of HIV-1 GAG trafficking in infected macrophages. PLoS Pathog. *4*, e1000015.

Hladik, F., and McElrath, M.J. (2008). Setting the stage: host invasion by HIV. Nat. Rev. Immunol. *8*, 447–457.

Honeycutt, J.B., Thayer, W.O., Baker, C.E., Ribeiro, R.M., Lada, S.M., Cao, Y., Cleary, R.A., Hudgens, M.G., Richman, D.D., and Garcia, J.V. (2017). HIV persistence in tissue macrophages of humanized myeloid-only mice during antiretroviral therapy. Nat. Med. *23*, 638–643.

Hübner, W., McNerney, G.P., Chen, P., Dale, B.M., Gordon, R.E., Chuang, F.Y., Li, X.D., Asmuth, D.M., Huser, T., and Chen, B.K. (2009). Quantitative 3D video microscopy of HIV transfer across T cell virological synapses. Science *323*, 1743–1747.

Hyun, J., Romero, L., Riveron, R., Flores, C., Kanagavelu, S., Chung, K.D., Alonso, A., Sotolongo, J., Ruiz, J., Manukyan, A., et al. (2015). Human intestinal epithelial cells express interleukin-10 through Toll-like receptor 4-mediated epithelial-macrophage crosstalk. J. Innate Immun. *7*, 87–101.

Iwami, S., Takeuchi, J.S., Nakaoka, S., Mammano, F., Clavel, F., Inaba, H., Kobayashi, T., Misawa, N., Aihara, K., Koyanagi, Y., and Sato, K. (2015). Cell-to-cell infection by HIV contributes over half of virus infection. eLife *4*, e08150.

Jolly, C., Kashefi, K., Hollinshead, M., and Sattentau, Q.J. (2004). HIV-1 cell to cell transfer across an Env-induced, actin-dependent synapse. J. Exp. Med. *199*, 283–293.

Keele, B.F., Giorgi, E.E., Salazar-Gonzalez, J.F., Decker, J.M., Pham, K.T., Salazar, M.G., Sun, C., Grayson, T., Wang, S., Li, H., et al. (2008). Identification and characterization of transmitted and early founder virus envelopes in primary HIV-1 infection. Proc. Natl. Acad. Sci. USA *105*, 7552–7557.

Kulpa, D.A., Brehm, J.H., Fromentin, R., Cooper, A., Cooper, C., Ahlers, J., Chomont, N., and Sékaly, R.P. (2013). The immunological synapse: the gateway to the HIV reservoir. Immunol. Rev. *254*, 305–325.

Liou, L.Y., Herrmann, C.H., and Rice, A.P. (2002). Transient induction of cyclin T1 during human macrophage differentiation regulates human immunodeficiency virus type 1 Tat transactivation function. J. Virol. *76*, 10579–10587.

Ma, Z.M., Dutra, J., Fritts, L., and Miller, C.J. (2016). Lymphatic Dissemination of Simian Immunodeficiency Virus after Penile Inoculation. J. Virol. *90*, 4093–4104.

Margolis, L., and Shattock, R. (2006). Selective transmission of CCR5-utilizing HIV-1: the 'gatekeeper' problem resolved? Nat. Rev. Microbiol. *4*, 312–317.

Martin, N., Welsch, S., Jolly, C., Briggs, J.A., Vaux, D., and Sattentau, Q.J. (2010). Virological synapse-mediated spread of human immunodeficiency virus type 1 between T cells is sensitive to entry inhibition. J. Virol. *84*, 3516–3527.

Miller, C.J., Alexander, N.J., Sutjipto, S., Lackner, A.A., Gettie, A., Hendrickx, A.G., Lowenstine, L.J., Jennings, M., and Marx, P.A. (1989). Genital mucosal transmission of simian immunodeficiency virus: animal model for heterosexual transmission of human immunodeficiency virus. J. Virol. *63*, 4277–4284.

Nasu, K., and Narahara, H. (2010). Pattern recognition via the toll-like receptor system in the human female genital tract. Mediators Inflamm. *2010*, 976024.

Ott, C., and Lippincott-Schwartz, J. (2012). Visualization of live primary cilia dynamics using fluorescence microscopy. Curr. Protoc. Cell Biol. *Chapter 4*, Unit 4.26.

Politch, J.A., Marathe, J., and Anderson, D.J. (2014). Characteristics and quantities of HIV host cells in human genital tract secretions. J. Infect. Dis. *210* (*Suppl 3*), S609–S615.

Pomerantz, R.J., Feinberg, M.B., Trono, D., and Baltimore, D. (1990). Lipopolysaccharide is a potent monocyte/macrophage-specific stimulator of human immunodeficiency virus type 1 expression. J. Exp. Med. *172*, 253–261.

Pudney, J., and Anderson, D.J. (1995). Immunobiology of the human penile urethra. Am. J. Pathol. *147*, 155–165.

Ribeiro Dos Santos, P., Rancez, M., Prétet, J.L., Michel-Salzat, A., Messent, V., Bogdanova, A., Couëdel-Courteille, A., Souil, E., Cheynier, R., and Butor, C. (2011). Rapid dissemination of SIV follows multisite entry after rectal inoculation. PLoS ONE *6*, e19493.

Rodrigues, V., Ruffin, N., San-Roman, M., and Benaroch, P. (2017). Myeloid Cell Interaction with HIV: A Complex Relationship. Front. Immunol. *8*, 1698.

Rudnicka, D., Feldmann, J., Porrot, F., Wietgrefe, S., Guadagnini, S., Prévost, M.C., Estaquier, J., Haase, A.T., Sol-Foulon, N., and Schwartz, O. (2009). Simultaneous cell-to-cell transmission of human immunodeficiency virus to multiple targets through polysynapses. J. Virol. *83*, 6234–6246.

Saïdi, H., Carbonneil, C., Magri, G., Eslahpazir, J., Sekaly, R.P., and Bélec, L. (2010). Differential modulation of CCR5-tropic human immunodeficiency virus-1 transfer from macrophages towards T cells under interleukin-4/interleukin-13 microenvironment. Hum. Immunol. *71*, 1–13.

Shen, R., Richter, H.E., Clements, R.H., Novak, L., Huff, K., Bimczok, D., Sankaran-Walters, S., Dandekar, S., Clapham, P.R., Smythies, L.E., and Smith, P.D. (2009). Macrophages in vaginal but not intestinal mucosa are monocyte-like and permissive to human immunodeficiency virus type 1 infection. J. Virol. *83*, 3258–3267.

Sigal, A., Kim, J.T., Balazs, A.B., Dekel, E., Mayo, A., Milo, R., and Baltimore, D. (2011). Cell-to-cell spread of HIV permits ongoing replication despite antiretroviral therapy. Nature *477*, 95–98.

Stanley, M.A. (2012). Epithelial cell responses to infection with human papillomavirus. Clin. Microbiol. Rev. *25*, 215–222.

Stevenson, M. (2015). Role of myeloid cells in HIV-1-host interplay. J. Neurovirol. *21*, 242–248.

Swingler, S., Mann, A.M., Zhou, J., Swingler, C., and Stevenson, M. (2007). Apoptotic killing of HIV-1-infected macrophages is subverted by the viral envelope glycoprotein. PLoS Pathog. *3*, 1281–1290.

Tudor, D., Yu, H., Maupetit, J., Drillet, A.S., Bouceba, T., Schwartz-Cornil, I., Lopalco, L., Tuffery, P., and Bomsel, M. (2012). Isotype modulates epitope specificity, affinity, and antiviral activities of anti-HIV-1 human broadly neutralizing 2F5 antibody. Proc. Natl. Acad. Sci. USA *109*, 12680–12685.

Wakabayashi, Y., Chua, J., Larkin, J.M., Lippincott-Schwartz, J., and Arias, I.M. (2007). Four-dimensional imaging of filter-grown polarized epithelial cells. Histochem. Cell Biol. *127*, 463–472.

Wang, L., Eng, E.T., Law, K., Gordon, R.E., Rice, W.J., and Chen, B.K. (2017). Visualization of HIV T cell virological synapses and virus-containing compartments by three-dimensional correlative light and electron microscopy. J. Virol. *91*, e01605-16.

Zhou, Z., Xu, L., Sennepin, A., Federici, C., Ganor, Y., Tudor, D., Damotte, D., Barry Delongchamps, N., Zerbib, M., and Bomsel, M. (2018). The HIV-1 viral synapse signals human foreskin keratinocytes to secrete thymic stromal lymphopoietin facilitating HIV-1 foreskin entry. Mucosal Immunol. *11*, 158–171.

Zussman, A., Lara, L., Lara, H.H., Bentwich, Z., and Borkow, G. (2003). Blocking of cell-free and cell-associated HIV-1 transmission through human cervix organ culture with UC781. AIDS *17*, 653–661.